colloids and interfaces

MDPI

Article

Spreading and Imbibition of Vesicle Dispersion Droplets on Porous Substrates

Abhijeet Kumar [1], Jochen Kleinen [2], Joachim Venzmer [2], Anna Trybala [3], Victor Starov [3] and Tatiana Gambaryan-Roisman [1,*]

1 Institute of Technical Thermodynamics, TU Darmstadt, 64287 Darmstadt, Germany
2 Research Interfacial Technology, Evonik Nutrition & Care GmbH, 45127 Essen, Germany
3 Department of Chemical Engineering, Loughborough University, Loughborough, LE11 3TU, UK
* Correspondence: gtatiana@ttd.tu-darmstadt.de; Tel.: +49-6151-162-2264

Received: 2 June 2019; Accepted: 12 July 2019; Published: 21 July 2019

Abstract: Vesicles have recently found widespread use in applications such as conditioning of textiles, paper and hair, as well as transdermal drug delivery. The mode of treatment in several such cases involves the application of droplets of aqueous dispersions of vesicles onto dry porous substrates like paper and textiles. One of the factors which affects the performance of such treatments is the rate at which the droplets spread and imbibe on the porous substrate. Depending upon the specific purpose of the treatment either a fast or slow droplet spreading kinetics could be desired. Therefore, it is important to have a good understanding of the droplet spreading process and the factors which influence it. In this work, an experimental investigation of the simultaneous spreading and imbibition of vesicle dispersion droplets on cellulose filter papers is carried out. Two different types of vesicles which are composed of similar lipid molecules but exhibit contrasting lipid bilayer phase behavior are used. Two different grades of filter papers with comparable porosities but different thicknesses are used as porous substrate. It is found that the droplet spreading behavior is of the "complete wetting" type on the thicker porous substrate, whereas it is of the "partial wetting" type on the thinner substrate. Furthermore, it is observed that the spreading of droplets containing vesicles with liquid-crystalline phase bilayers occurs faster than that of vesicles with solid-gel phase bilayers. The secondary radial penetration which commences after the initial droplet spreading is complete is also investigated and discussed.

Keywords: vesicles; wetting; imbibition

1. Introduction

The process of simultaneous spreading and imbibition of droplets of Newtonian and non-Newtonian liquids on dry porous substrates is relevant in several applications such as inkjet printing [1], dried spot sampling of blood and other biological liquids [2,3], softening of paper and textiles [4] and transdermal delivery of drugs and cosmetic ingredients [5,6]. The mechanism of such spreading processes has been investigated in earlier works for Newtonian liquids like water, silicone oil [7,8], and more recently also for non-Newtonian complex liquids like blood [9,10]. However, not much is known about the the spreading behavior on dry porous substrates of vesicle dispersions which form a commercially important class of complex liquids. Considering the widespread interest in use of vesicle dispersions in conditioning and topical drug delivery applications where they are sprayed onto porous substrates like paper, textile [11,12], hair [13] and human skin [14,15], it is important that their spreading behavior on such porous substrates be well understood.

When liquid droplets loaded with active ingredients are sprayed onto a porous substrate with the goal of attaining a certain desired end result, the efficiency among several factors is influenced by the kinetics of droplet spreading and imbibition. Depending upon the purpose of the treatment either a fast or a slow rate of droplet spreading and imbibition could be desirable. A practical example is the industrial surface modification of paper sheets or textiles where an aqueous dispersion of softening ingredients is sprayed onto dry or partially wet sheets and subsequently dried before being spooled onto rolls at high speeds, as shown schematically in Figure 1. For a superior softening result, it is desirable that most of the softening ingredients are deposited on the external substrate surfaces which could be achieved by minimizing the penetration of the liquid softening formulation into the porous substrate. Therefore, it is very important to have a good understanding of the kinetics of the spreading process.

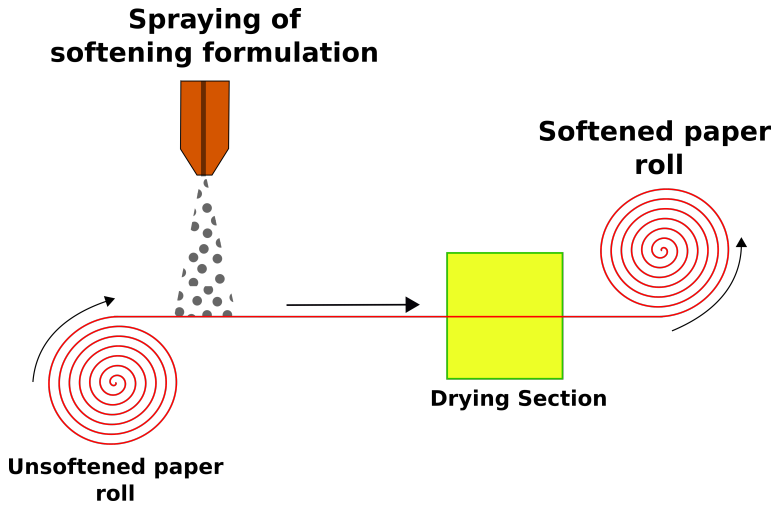

Figure 1. Schematic representation of a typical paper softening process as carried out in industries.

The spreading process kicks off once the droplets contact the porous substrate, and typically proceeds with the formation of a liquid cap over the porous substrate and simultaneous imbibition-driven liquid penetration into the porous substrate, as shown schematically in Figure 2. The kinetics of the process is characterized in terms of the rates of variation of spreading parameters, namely, the base radius ($L(t)$) and dynamic contact angle of the liquid cap ($\theta(t)$) and radius of the wetted region ($l(t)$) [7]. The spreading kinetics is typically governed by the porous substrate's structure, the wettability of solid surfaces by the liquid and the liquid's rheological properties. Other physico-chemical interaction between the dispersion and the substrate such as adsorption, blockage of pores could also be important [16]. The effect of gravity could be neglected for low droplet volumes and small pores where the Bond number, Bo, describing the ratio of gravitational to capillary forces, is much less than 1. After the primary wetting process involving simultaneous spreading and imbibition, comes to an end, further radial penetration of liquid has been reported [17]. The secondary penetration has been explained to occur due to competitive spreading between pores in the porous substrate until equilibrium is attained [17]. The extent of secondary radial liquid penetration has also been investigated in our experiments.

In previous works, based on the characteristic trends observed in time variation of spreading parameters, such droplet spreading processes have been classified qualitatively into two types, namely, the partial and complete wetting cases [10]. The mode of variation of spreading parameters which determines whether the spreading process is of the complete or the partial wetting type has been shown schematically in Figure 3A,B. In earlier works [7–9], the spreading behavior exhibiting three phases (A, B, C) has been observed for partially wetting liquids (water), whereas the behavior with only two phases has been observed for completely wetting liquids.

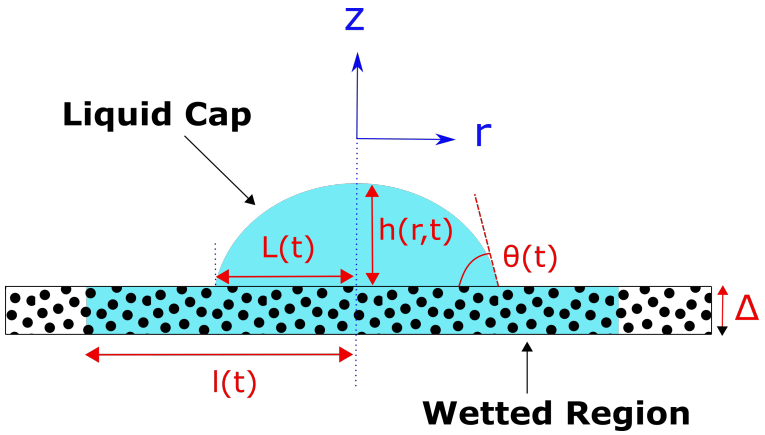

Figure 2. Schematic representation of the simultaneous droplet spreading and imbibition process.

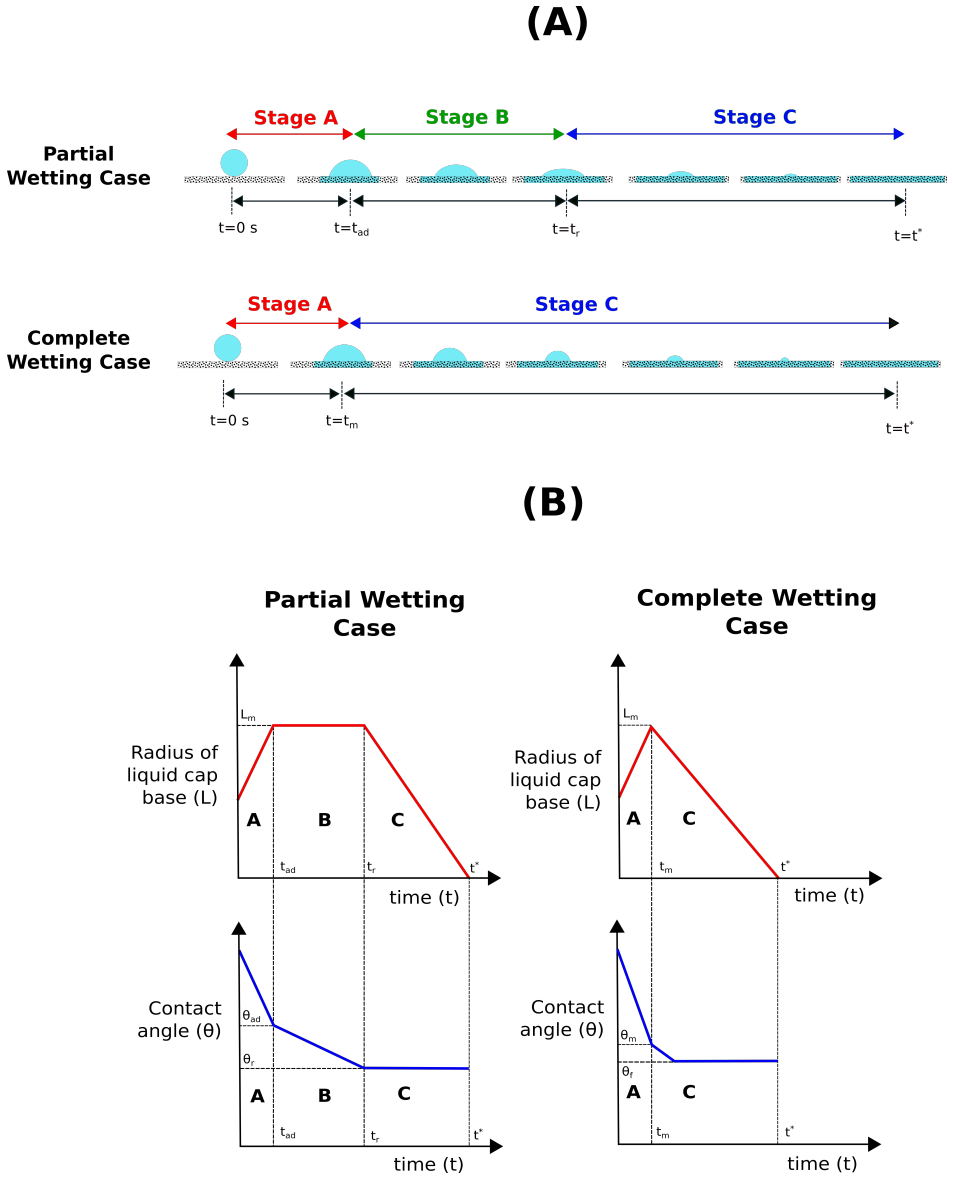

Figure 3. (**A**) Schematic representation of different stages of the droplet spreading and imbibition for the partial wetting case and for the complete wetting case. (**B**) Characteristic trends in variation of the spreading parameters, L (liquid cap base radius) and θ (contact angle) in the cases of partial (left) and complete (right) wetting during the primary spreading phase.

In the partial wetting case, the overall primary spreading process could be divided into three stages A, B and C, as shown in Figure 3A,B. Stage A involves a rapid spreading of the droplet on the porous substrate until the liquid cap base radius, $L(t)$, reaches its maximum value L_m and the dynamic contact angle, $\theta(t)$, reaches the advancing contact angle value of θ_{ad}. In stage B, $L(t)$ remains fixed at L_m while $\theta(t)$ decreases from θ_{ad} to the receding contact angle, θ_r. In stage C, $\theta(t)$ remains fixed at θ_r while $L(t)$ decreases from L_m to zero. The partial wetting case is characterized by the presence of Phase B in which the liquid cap base remains pinned and results in a contact angle hysteresis.

The complete wetting case characterized by the non-existence of Stage B (as shown in Figure 3A,B). In this case, as the liquid cap base radius, $L(t)$ reaches its maximum value of L_m at the end of Stage A, the liquid cap starts receding almost instantaneously without being pinned. Furthermore, as the liquid cap base recedes during Phase C, the contact angle, $\theta(t)$, remains constant at a certain value of θ_f.

In this work, an experimental investigation of the spreading of aqueous vesicle dispersion droplets on cellulose filter papers has been carried out. The primary objective of the work is to elucidate the characteristics of the spreading process and to identify the vesicle and porous substrate properties which affect the droplet spreading kinetics. This is accomplished by varying the vesicle dispersion and porous substrates in the spreading experiments. Two different types of vesicle dispersions composed of lipids exhibiting contrasting lipid bilayer phase behavior and two filter papers with different thicknesses but comparable porosities are used.

The two vesicle types used in the study are composed of the lipids Rewoquat® WE 18 and Rewoquat® WE 15, respectively. The chemical structures of the two lipids are shown in Figure 4A. Both of these lipids belong to the family of esterquats which are used commonly in formulations for softening of paper and textiles [13]. Although these vesicles have similar sizes and zeta potentials, they differ in terms of the phase behavior of constituent lipid bilayers. While the lipid bilayers constituting WE18 vesicles exist in the solid-gel phase, they exist in the liquid-crystalline phase in WE15 vesicles [12]. Using these vesicles provides us the opportunity to identify if the lipid bilayer phase behavior affects the spreading behavior of vesicle dispersion droplets. Furthermore, in order to investigate the effect of porous substrate structure on the spreading process, two different types of filter papers, namely, Whatman 903 and Sartorius 388 were used as porous substrate.

This paper is organized into a total of 5 sections. After this introduction, the materials and methods are described. After that, the characteristic experimental trends with which the type of the spreading process—that is, partial or complete wetting case—are identified are discussed. Thereafter, the experimental results obtained in different cases for the temporal variation of spreading parameters, namely, the liquid cap base radius ($L(t)$), dynamic contact angle ($\theta(t)$) and radius of the wetted region ($l(t)$) are presented. The spreading behavior of vesicle dispersion droplets is found to be of the "complete wetting" type on Whatman 903 filter paper and of the "partial wetting" type on Sartorius 388 filter papers. The spreading kinetics of the WE 15 vesicle dispersions is found to be faster than that of WE 18 vesicle dispersions on both the filter papers. The experimental results are scaled in non-dimensionalized form using the theory proposed by Chao et al. [10] and compared with each other.

2. Materials and Methods

2.1. Preparation and Characterization of Vesicles

The two types of vesicles used in this study were composed of the lipids, Rewoquat WE18 and Rewoquat WE15, respectively. The chemical structures of the lipid molecules have been shown in Figure 4A. The mass concentration of lipids in both the vesicle dispersions was approx. 8 wt.%. The preparation of these vesicles involved the initial preparation of large vesicles via the melt dispersion method which was followed by high-pressure homogenization for size reduction. The method of preparation of these vesicles has been described in detail in our previous works [11,12].

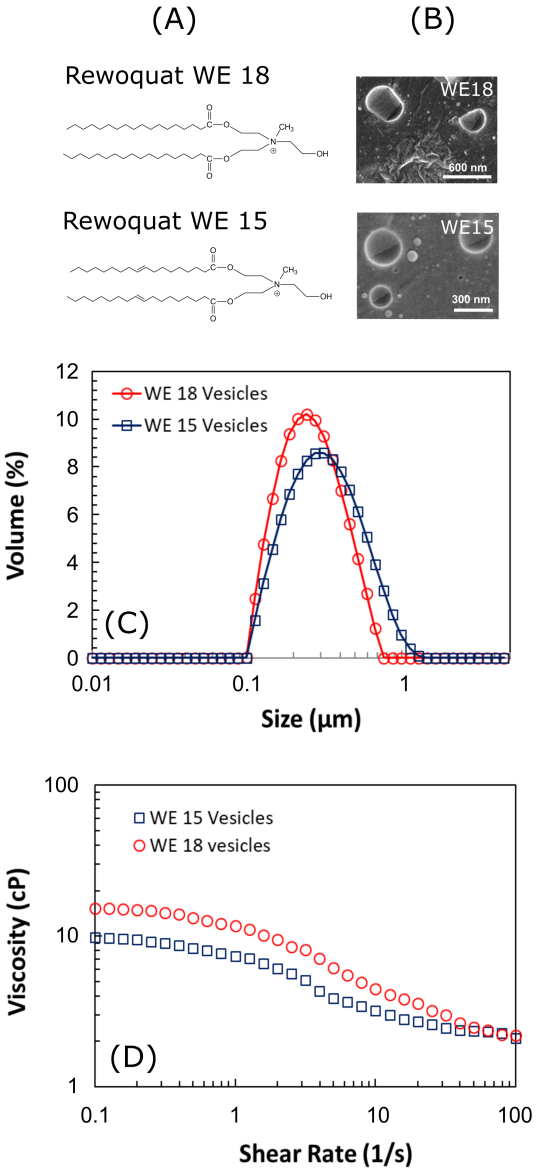

Figure 4. (**A**) Chemical structures of the lipids Rewoquat WE18 and WE15; (**B**) Cryo-electron microscopy (EM) images of WE18 and WE15 vesicles; (**C**) Particle size distributions of WE18 and WE15 vesicles; (**D**) Variation of the viscosity of WE18 and WE15 vesicle dispersions with shear rate.

The vesicles were visualized directly via cryo-electron microscopy (EM) after sample preparation via high pressure bulk freezing and freeze-fracture (see Figure 4B) [17]. The size distributions of the vesicle dispersions as obtained via laser diffraction using the Malvern Mastersizer 3000 laser diffraction particle size analyzer have been shown in Figure 4C [12].

The rheology of the vesicle dispersions was characterized via viscosity measurements at different shear rates (0.1 to 100 s^{-1}) using the AR-G2 rheometer from TA Instruments. The viscosity vs. shear rate profiles of both WE18 and WE15 vesicle dispersions have been shown in Figure 4D.

The vesicle zeta potentials were determined via electrophoretic mobility characterization on a Malvern Zetasizer Nano ZS. A detailed account of the vesicle zeta potential measurements has been provided in our earlier work [12].

2.2. Porous Substrate

Commercial cellulose fiber filter papers, namely, Whatman 903 and Sartorius 388, were used as porous substrates for the spreading experiments. The filter papers were observed using a optical laser scanning microscope from Keyence (see Figure 5). The filter paper thicknesses were obtained from cross-sectional images of the filter papers.

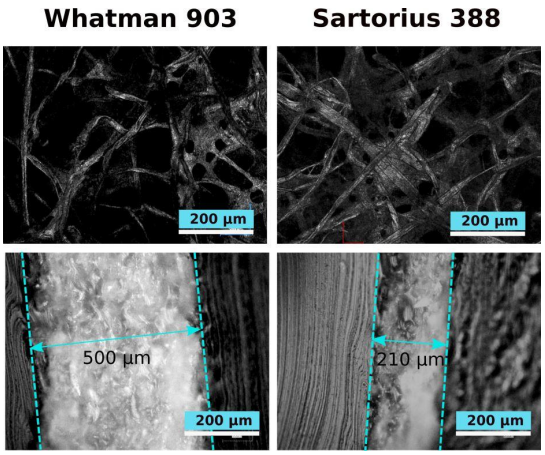

Figure 5. Images of the top surfaces (first row) and cross-sections (second row) of the filter papers, Whatman 903 and Sartorius 388, used in the spreading experiments

2.3. Spreading Experiments

The simultaneous spreading and imbibition of liquid droplets on porous substrates is observed using an experimental setup as shown schematically in Figure 6. The liquid cap which is formed over the porous substrate is imaged from the side using a high speed camera (i-Speed LT from Olympus). The wetted area formed inside the porous substrate due to imbibition is simultaneously imaged using a camera from the top (Pike F-032 from Allied Vision). The liquid droplets with volume of 10 ± 0.5 µL were produced using a syringe pump (Nanomite from Harvard Apparatus) and were gently dropped on the porous substrate from a negligible height. A set of images obtained in a particular experiment from the top-view and side-view cameras have been shown in Figure 7. Each spreading experiment was conducted thrice to ensure the reproducibility of the results. The values of the spreading parameters ($L(t)$, $l(t)$ and $\theta(t)$) were measured directly from the recorded images using the open source image analysis software ImageJ.

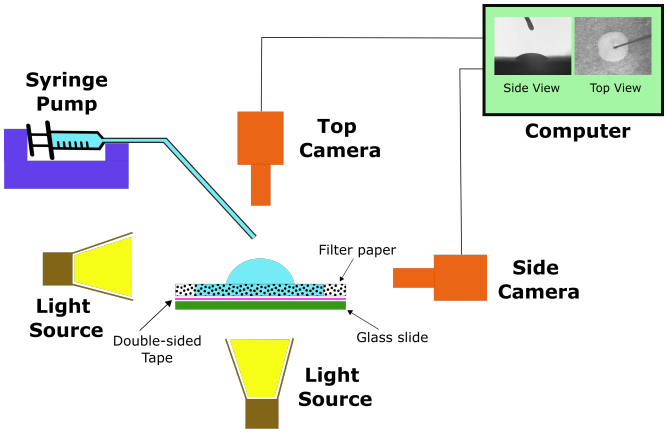

Figure 6. Sketch of the experimental setup used for the droplet spreading experiments.

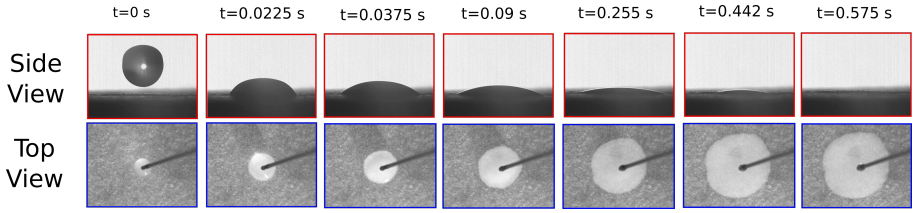

Figure 7. Evolution of the liquid cap and the wetted area with time for the spreading of a WE18 droplet on a Sartorius 388 filter paper, as observed from the side and top cameras, respectively. The dimensions of the side view and the top view images are 7.4 mm × 5.6 mm and 18.3 mm × 13.8 mm, respectively.

3. Results and Discussion

3.1. Vesicle Dispersion Properties

The average sizes of WE15 and WE18 vesicles as obtained from the size distributions are 0.27 µm and 0.35 µm, respectively. A significant difference between the two vesicles is that the lipids bilayers in WE18 vesicles exist in the solid-gel phase, whereas they exist in the liquid-crystalline phase in WE15 vesicles [12]. This leads to a difference in the shapes of the vesicles with WE15 vesicles being round and smoothly shaped and WE18 vesicles existing as polyhedrons with sharp edges [18]. The contrasting shapes of the vesicles could be identified from their cryo-EM images shown in Figure 4B. The zeta potentials of the vesicles were found to be +60 mV (±10 mV) for both WE18 and WE15 vesicles. Furthermore, it could be identified that both the dispersions behave as shear thinning complex liquids with the viscosity of the WE18 vesicle dispersion being higher than that of the WE15 vesicle dispersion in the shear rate range of 0.1 to 100 s^{-1} (Figure 4D). As the viscosity of the liquid is an important parameter governing spreading kinetics, it could lead to differences in the spreading kinetics of WE18 and WE15 droplets on filter papers [7].

3.2. Filter Paper Characteristics

As observed from the cross-sectional images (Figure 5), the thicknesses of Whatman 903 and Sartorius 388 are 500 µm and 210 µm, respectively. The porosities of the filter papers were estimated from their grammage (mass per unit area) and thickness values and are found to be 0.50 and 0.57 for Whatman 903 and Sartorius 388, respectively (see supporting information). The porosity of Sartorius 388 is only slightly higher than that of Whatman 903. The spreading of liquid droplets on Whatman 903 was investigated in an earlier work, where the spreading behavior was found to be of the complete wetting type [9]. The spreading behavior on Sartorius 388 has not yet been reported. Differences between the spreading behavior of droplets on the two filter papers would help identify how the porous substrate thickness affects spreading.

3.3. Droplet Spreading Kinetics

The variation of the spreading parameters with time, $L(t)$, $l(t)$ and $\theta(t)$, as obtained in the experiments is plotted in Figure 8. The most important observation from Figure 8 is the intrinsic difference in droplet spreading characteristics on the two porous substrates. It is observed that the spreading behavior of both WE15 and WE18 vesicle dispersion droplets is of the complete wetting type on Whatman 903, while it is of the partial wetting type on Sartorius 388. For the same droplet volume, the final size of the wetted area formed on Sartorius 388 is larger than that on Whatman 903 due to it's lower thickness and hence lower pore space available per unit substrate area.

Furthermore, the time required for full imbibition of the droplets into the porous substrate is much shorter for Whatman 903 than that for Sartorius 388. As the pore sizes of the two substrates are comparable, the difference in spreading behavior could be attributed to the larger thickness of Whatman 903. The larger thickness of Whatman 903 leads to an higher rate of liquid penetration into the porous substrate due to imbibition. It can be suggested that the higher rate of liquid penetration

into the porous substrate leads to complete wetting behavior in the case of Whatman 903. On the other hand, due to the slower liquid penetration rate, the wetting behavior on Sartorius 388 is of the partial wetting type.

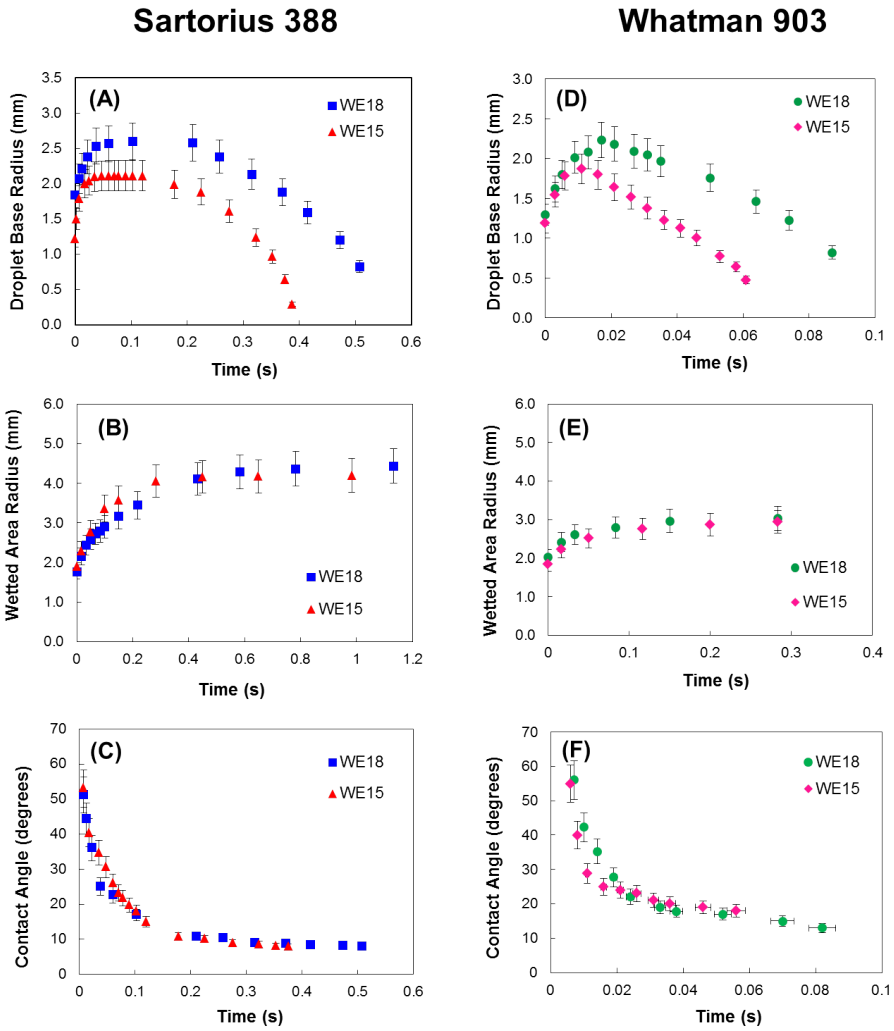

Figure 8. Evolution of the liquid cap base radius, the wetted area radius and the contact angle with time for the spreading of WE18 and WE15 droplets on Sartorius 388 (**A**–**C**) and Whatman 903 (**D**–**F**).

The second important observation from Figure 8 is the difference between spreading kinetics of WE18 and WE15 droplets. It is observed that the spreading of WE15 droplets is faster than that of WE18 droplets on both Whatman 903 and Sartorius 388. As the difference in phase behavior of lipid bilayers inside the vesicles has no effect on capillary forces, the difference in spreading kinetics can be attributed to the difference in viscosities of the two vesicle dispersions which could be identified from Figure 4D. Given that the capillary forces are unchanged, the liquid with lower viscosity penetrates into the porous substrate faster [19]. As a result the imbibition of WE15 liquid occurs faster than the imibition of WE18 liquid. A similar result was observed in an earlier work involving blood droplets where the blood droplet with higher viscosity was found to spread and imbibe slower on the substrate [20]. However, a difference in the maximum liquid cap base radius—L_m—attained during the spreading process is observed with respect to the results of Chao et al. [20]. In our experiments, it has been found that L_m is larger for WE18 droplets with higher viscosity than that for WE15 droplets with lower viscosity. This effect can be attributed to the slower imbibition kinetics of WE18 liquid which allows the liquid cap more time to spread in the case of WE18.

3.4. Non-Dimensionalized Droplet Spreading Kinetics

The spreading parameters—$L(t)$, $l(t)$ and $\theta(t)$—and the spreading time—t—are non-dimensionalized according to the method described by Chao et al. [10] and plotted as shown in Figure 9. The liquid cap base radius and the wetted area radius are non-dimensionalized with respect to their maximum values. The time required for complete imibition of the liquid cap was used as denominator for non-dimensionalizing the spreading time. It can be identified from Figure 9 that the non-dimensionalized spreading kinetics of WE18 and WE15 droplets are identical on Sartorius 388 and Whatman 903. This confirms that the physical phenomena governing the spreading of WE18 and WE15 droplets are identical for both the liquids. The observed differences in spreading kinetics are thus only a result of the difference in rheological properties of the vesicle dispersions.

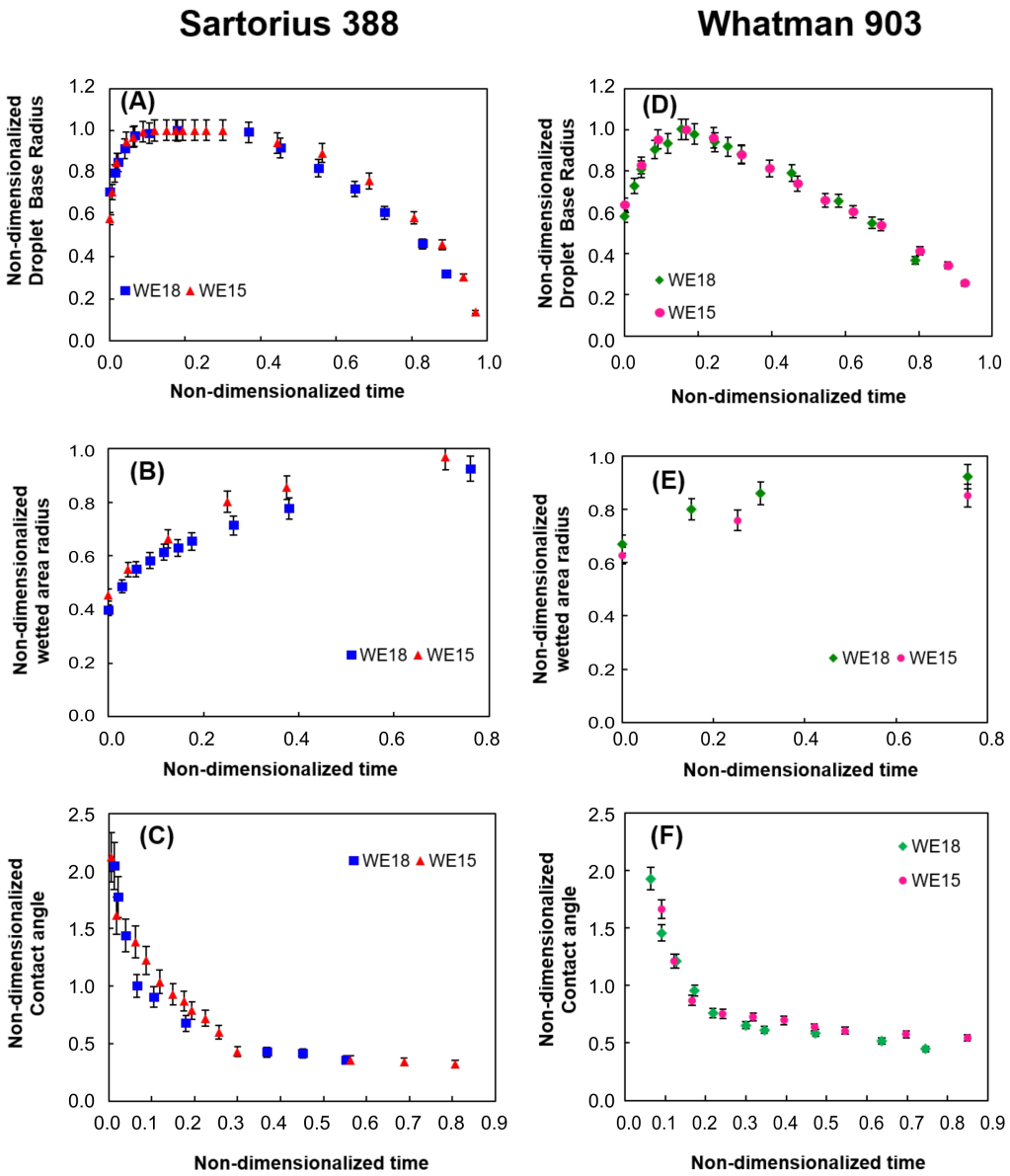

Figure 9. Evolution of the dimensionless liquid cap base radius, the dimensionless wetted area radius and the non-dimensionallzed contact angle with non-dimensionalied time for the spreading of WE18 and WE15 droplets on Sartorius 388 (**A**–**C**) and Whatman 903 (**D**–**F**).

3.5. Secondary Radial Liquid Penetration

The secondary radial penetration of the liquid occurs after the liquid cap has disappeared over the substrate and is shown schematically on Figure 10A. The wetted areas observed right after the primary spreading phase in which the liquid cap disappers and after equilibrium has been reached are shown for the different liquid-substrate combinations on Figure 10B. Apart from the WE18 and WE15 vesicle dispersions, the secondary penetration of water droplets was investigated as well. The ratio of the equilibrium wetted area to the intermediate wetted area which provides a measure of the extent of secondary liquid penetration is enlisted on Table 1 for the different cases.

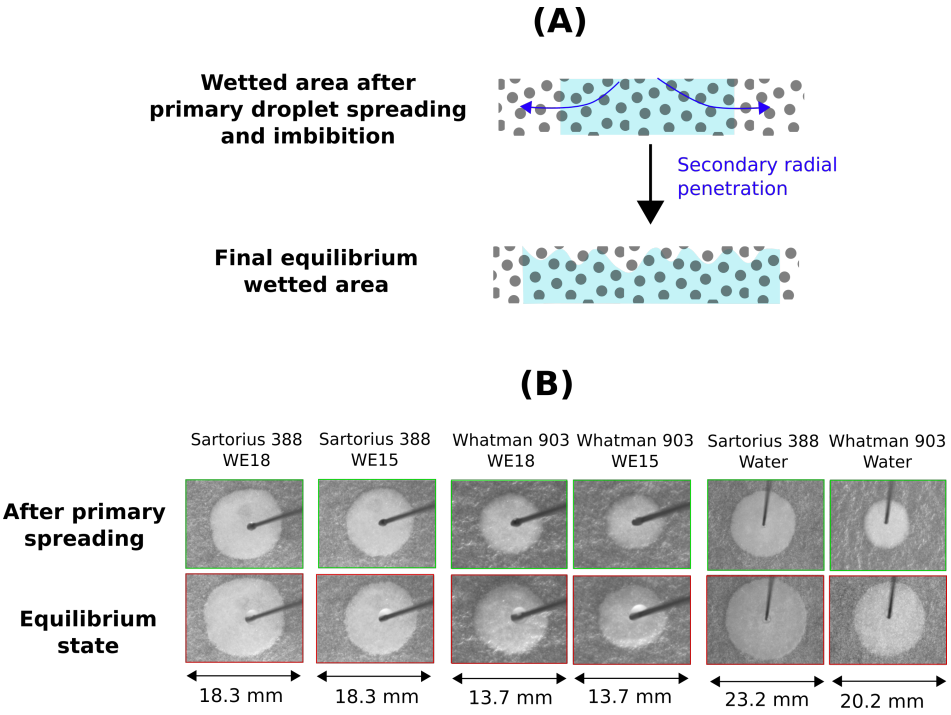

Figure 10. (**A**) Schematic representation of secondary radial liquid penetration, (**B**) Wetted areas observed right after the disappearance of the liquid cap and after equilibrium has been reached for different liquid-substrate combinations

Table 1. Secondary radial penetration of water, WE18 and WE15 vesicle dispersions on Sartorius 388 and Whatman 903.

Liquid Type	Ratio of Final to Intermediate Wetted Area Diameters	
	Sartorius 388	Whatman 903
Water	1.23	1.55
WE18	1.11	1.18
WE15	1.08	1.17

It could be observed from Table 1 that the extent of secondary liquid penetration is higher on Whatman 903 than on Sartorius 388 for all the liquids. Among the liquids, the extent of secondary liquid penetration is highest for water followed by both WE18 and WE15 which are comparable. The above observations indicates that the extent of secondary liquid penetration is dependent on both substrate thickness as well as liquid viscosity. The primary driving force for secondary liquid penetration is the lower capillary forces of liquid meniscii in pores existing at the periphery of the wetted area. A higher substrate thickness therefore leads to a larger number of pores and hence a higher capillary force which pulls out the liquid in the radial direction and hence results in greater secondary spreading. The peripheral region gets filled at the expense of liquid from the center. In addition, as a liquid with high viscosity would not flow easily under the action of the radial capillary forces, WE18

and WE15 vesicle dispersions with higher viscosities exhibit much lower secondary liquid penetration compared to water.

3.6. Significance of the Results to Softening Treatment of Paper

A schematic representation of the typical industrial process for softening treatment of dry paper sheets is shown in Figure 1. During the treatment, the spraying of liquid droplets containing vesicles on dry paper sheets is typically followed by a fast and intensive drying process. In a typical softening treatment deposition on external surfaces is preferred over deposition on internal surfaces. This could be done by minimizing the penetration of softening formulation into the porous substrate by keeping the time gap between spraying and drying stages (Δt) much lower than the total time required for the liquid droplets to penetrate into the substrate. In order to keep the time gap as low as possible, the paper sheets are typically moved at very high speeds between the spraying and drying sections. However, with a better understanding of droplet spreading kinetics, the time gap, Δt, could be optimized such that the droplet is dried when the base radius of the liquid cap is at its maximum as shown in Figure 8A. This would lead to the softening ingredients being deposited on the external substrate surface with the greatest possible coverage. It is evident that the optimum time gap (Δt) depends on the properties of the porous substrate such as its thickness and porosity as well as the properties of the liquid formulation.

4. Conclusions

In this work are investigated the simultaneous spreading and imbibition of vesicle dispersion droplets on porous cellulose fiber filter papers. Two porous substrates of comparable porosity but different thicknesses (500 μm and 210 μm) were used. Two vesicles dispersions containing sub-micron size vesicles which are composed of chemically similar lipids but exhibit contrasting lipid bilayer phase behavior are used. It is shown that the spreading behavior of vesicle dispersions on porous substrates is strongly influenced by the thickness of the porous substrate as well as the phase behavior of the lipid bilayers constituting the vesicles. Droplet spreading behavior is of the complete wetting type on Whatman 903 which has a thickness of 500 μm, while it is of the partial wetting type on Sartorius 388 which has a thickness of 210 μm. On both the filter papers, the spreading kinetics of the liquid droplets containing WE18 vesicles with solid-gel phase bilayers is slower than that of liquid droplets containing WE15 vesicles with liquid-crystalline phase bilayers. It is shown that the faster spreading kinetics of WE15 vesicles is due to its lower viscosity which results in a faster rate of liquid penetration into the porous substrate via imbibition. In our earlier works, we demonstrated using electrokinetic techniques how the bilayer phase behavior of vesicles influences deposition on porous and non-porous cellulose substrates [11,12,20,21]. In the present work, we take it a step further and show that it also influence the spreading kinetics of droplets on porous substrates. A good understanding of the droplet spreading kinetics could be useful in real-life applications such the softening treatment of paper, where the process parameters could be optimized to attain much better results.

Author Contributions: Conceptualization, A.K., V.S. and T.G.-R.; methodology, J.K., J.V., A.T. and V.S.; validation, V.S. and T.G.-R.; investigation, A.K. and A.T.; writing–original draft preparation, A.K.; writing–review and editing, J.K., J.V., A.T., V.S. and T.G.-R.; supervision, J.V. and T.G.-R.; project administration, T.G.-R.; funding acquisition, T.G.-R.

Funding: This research was funded by European Commission in the framework of Marie Curie Initial Training Network "Complex Wetting Phenomena" (CoWEt), grant agreement number 607861.

Conflicts of Interest: The authors declare no conflict of interest

References

1. Daniel, R.C.; Berg, J.C. Spreading on and penetration into thin, permeable print media: Application to ink-jet printing. *Adv. Colloid Interface Sci.* **2006**, *123–126*, 439–469. [CrossRef] [PubMed]

2. Li, W.; Tse, F.L. Dried blood spot sampling in combination with LC-MS/MS for quantitative analysis of small molecules. *Biomed. Chromatogr.* **2010**, *24*, 49–65. [CrossRef] [PubMed]
3. Li, W.; Tse, F.L. Dried blood spots as a sample collection technique for the determination of pharmacokinetics in clinical studies: considerations for the validation of a quantitative bioanalytical method. *Anal. Chem.* **2009**, *81*, 1557–1563.
4. Puchta, R. Cationic surfactants in laundry detergents and laundry aftertreatment aids. *J. Am. Oil Chem. Soc.* **1984**, *61*, 367–376. [CrossRef]
5. Ibrahim, S.A. Spray-on transdermal drug delivery systems. *Expert Opin. Drug Deliv.* **2015**, *12*, 195–205. [CrossRef] [PubMed]
6. Nayak, A.; Das, D.B.; Chao, T.C.; Starov, V.M. Spreading of a lidocaine formulation on microneedletreated Skin. *J. Pharm. Sci.* **2015**, *104*, 4109–4116. [CrossRef] [PubMed]
7. Starov, V.; Kostvintsev, S.; Sobolev, V.; Velarde, M.; Zhdanov, S. Spreading of liquid drops over dry porous layers: Complete wetting case. *J. Colloid Interface Sci.* **2002**, *252*, 397–408. [CrossRef] [PubMed]
8. Lee, K.; Cheah, C.; Copleston, R.; Starov, V.; Sefiane, K. Spreading and evaporation of sessile droplets: Universal behaviour in the case of complete wetting. *Colloids Surf. A Physicochem. Eng. Asp.* **2008**, *323*, 63–72. [CrossRef]
9. Chao, T.C.; Arjmandi-Tash, O.; Das, D.B.; Starov, V.M. Spreading of blood drops over dry porous substrate: Complete wetting case. *J. Colloid Interface Sci.* **2015**, *446*, 218–225. [CrossRef]
10. Chao, T.C.; Arjmandi-Tash, O.; Das, D.B.; Starov, V.M. Simultaneous spreading and imbibition of blood droplets over porous substrates in the case of partial wetting. *Colloids Surf. A Physicochem. Eng. Asp.* **2016**, *505*, 9–17. [CrossRef]
11. Kumar, A.; Gilson, L.; Henrich, F.; Dahl, V.; Kleinen, J.; Gambaryan-Roisman, T.; Venzmer, J. Intact deposition of cationic vesicles on anionic cellulose fibers: Role of vesicle size, polydispersity, and substrate roughness studied via streaming potential measurements. *J. Colloid Interface Sci.* **2016**, *473*, 152–161. [CrossRef] [PubMed]
12. Kumar, A.; Dahl, V.; Kleinen, J.; Gambaryan-Roisman, T.; Venzmer, J. Influence of lipid bilayer phase behavior and substrate roughness on the pathways of intact vesicle deposition: A streaming potential study. *Colloids Surf. A Physicochem. Eng. Asp.* **2017**, *521*, 302–311. [CrossRef]
13. Venzmer, J. Alltaegliche phanomene. Grenzflachenchemische Spezialitaeten. *Chemie in Unserer Zeit* **2008**, *42*, 72–79. [CrossRef]
14. Wang, S.; Zeng, D.; Niu, J.; Wang, H.; Wang, L.; Li, Q.; Li, C.; Song, H.; Chang, J.; Zhang, L. Development of an efficient transdermal drug delivery system with tat-conjugated cationic polymeric lipid vesicles. *J. Mater. Chem. B* **2014**, *2*, 877–884. [CrossRef]
15. Lohani, A.; Verma, A. Vesicles: Potential nano carriers for the delivery of skin cosmetics. *J. Cosmet. Laser Ther.* **2017**, *19*, 485–493. [CrossRef] [PubMed]
16. Arjmandi-Tash, O.; Kovalchuk, N.M.; Trybala, A.; Kuchin, I.V.; Starov, V. Kinetics of wetting and spreading of droplets over various substrates. *Langmuir* **2017**, *33*, 4367–4385. [CrossRef] [PubMed]
17. Jarl, B. Rosenholm. Liquid spreading on solid surfaces and penetration into porous matrices: Coated and uncoated papers. *Adv. Colloid Interface Sci.* **2015**, *220*, 8–53.
18. Kumar, A.; Kleinen, J.; Gambaryan-Roisman, T.; Venzmer, J. Electrokinetic investigation of deposition of cationic fabric softener vesicles on anionic porous cotton fabrics. *J. Colloid Interface Sci.* **2018**, *514*, 132–145. [CrossRef]
19. Gambaryan-Roisman, T. Liquids on porous layers: Wetting, imbibition and transport processes. *Curr. Opin. Colloid Interface Sci.* **2014**, *19*, 320–335. [CrossRef]
20. Chao, T.C.; Trybala, A.; Starov, V.; Das, D.B. Influence of haematocrit level on the kinetics of blood spreading on thin porous medium during dried blood spot sampling. *Colloids Surf. A Physicochem. Eng. Asp.* **2014**, *451*, 38–47. [CrossRef]
21. Kumar, A.; Kleinen, J.; Venzmer, J.; Gambaryan-Roisman, T. Effect of geometry on electrokinetic characterization of solid surfaces. *Langmuir* **2017**, *30*, 7556–7568. [CrossRef] [PubMed]

© 2019 by the authors. Licensee MDPI, Basel, Switzerland. This article is an open access article distributed under the terms and conditions of the Creative Commons Attribution (CC BY) license (http://creativecommons.org/licenses/by/4.0/).